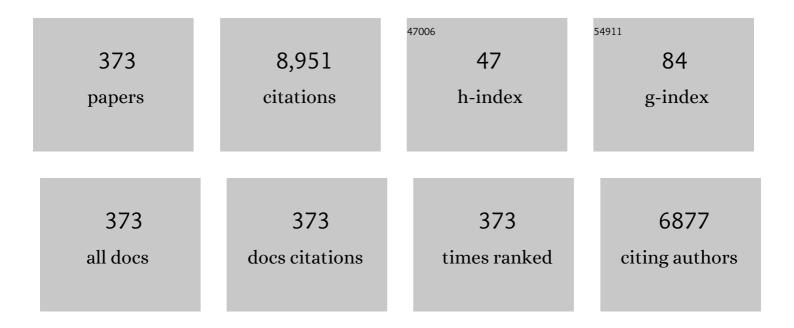
List of Publications by Year in descending order

Source: https://exaly.com/author-pdf/8510851/publications.pdf Version: 2024-02-01



#	Article	IF	CITATIONS
1	A Compact 112-Gbaud PAM-4 Silicon Photonics Transceiver for Short-Reach Interconnects. Journal of Lightwave Technology, 2022, 40, 2265-2273.	4.6	14
2	Integrated scanning spectrometer with a tunable micro-ring resonator and an arrayed waveguide grating. Photonics Research, 2022, 10, A74.	7.0	11
3	C-band 67â€GHz silicon photonic microring modulator for dispersion-uncompensated 100 Gbaud PAM-4. Optics Letters, 2022, 47, 2935.	3.3	21
4	Broadband high-Q multimode silicon concentric racetrack resonators for widely tunable Raman lasers. Nature Communications, 2022, 13, .	12.8	15
5	Photonic integrated circuits with bound states in the continuum: erratum. Optica, 2022, 9, 683.	9.3	1
6	40 GHz waveguide-integrated two-dimensional palladium diselenide photodetectors. Applied Physics Letters, 2022, 120, .	3.3	4
7	Large-Scale and Broadband Silicon Nitride Optical Phased Arrays. IEEE Journal of Selected Topics in Quantum Electronics, 2022, 28, 1-10.	2.9	22
8	Integrated Multimode Waveguide With Photonic Lantern for Speckle Spectroscopy. IEEE Journal of Quantum Electronics, 2021, 57, 1-8.	1.9	16
9	40 G III-V photodetectors on a monolithic InP/SOI platform. , 2021, , .		1
10	Inverse design of multi-band and wideband waveguide crossings. Optics Letters, 2021, 46, 884.	3.3	17
11	Optimal Bezier curve transition for low-loss ultra-compact S-bends. Optics Letters, 2021, 46, 876.	3.3	14
12	Nonparaxial Mode-Size Converter Using an Ultracompact Metamaterial Mikaelian Lens. Journal of Lightwave Technology, 2021, 39, 2077-2083.	4.6	9
13	Telecom InP-based quantum dash photodetectors grown on Si. Applied Physics Letters, 2021, 118, .	3.3	11
14	Fabrication-Tolerant and Low-Loss Hybrid Plasmonic Slot Waveguide Mode Converter. Journal of Lightwave Technology, 2021, 39, 2106-2112.	4.6	3
15	Tandem Configuration of Microrings and Arrayed Waveguide Gratings for a High-Resolution and Broadband Stationary Optical Spectrometer at 860 nm. ACS Photonics, 2021, 8, 1251-1257.	6.6	20
16	Guest Editorial Introduction to the JSTQE Issue on Advanced Photonic Modulation: Devices, Systems & Techniques. IEEE Journal of Selected Topics in Quantum Electronics, 2021, 27, 1-3.	2.9	0
17	Ultraâ€Narrowband Photodetector with High Responsivity Enabled by Integrating Monolayer Jâ€Aggregate Organic Crystal with Graphene. Advanced Optical Materials, 2021, 9, 2100158.	7.3	15
18	Compact High Resolution Speckle Spectrometer by Using Linear Coherent Integrated Network on Silicon Nitride Platform at 776 nm. Laser and Photonics Reviews, 2021, 15, 2100039.	8.7	22

#	Article	IF	CITATIONS
19	Near-infrared frequency comb generation from a silicon microresonator. Journal of Optics (United) Tj ETQq1 1 0.7	84314 rgB 2.2	Ţ/Overlock
20	High-performance III-V photodetectors on a monolithic InP/SOI platform. Optica, 2021, 8, 1204.	9.3	33
21	Investigation of low-power comb generation in silicon microresonators from dual pumps. Journal of Optics (United Kingdom), 2021, 23, 10LT03.	2.2	3
22	Subwavelength Silicon Photonics. Topics in Applied Physics, 2021, , 285-321.	0.8	0
23	1.3 μm regrown quantum-dot distributed feedback lasers on (001) Si: a pathway to scale towards 1 Tbit/s. , 2021, , .		1
24	Raman Lasing in Multimode Silicon Racetrack Resonators. Laser and Photonics Reviews, 2021, 15, 2000336.	8.7	21
25	High-extinction CROW filters for scalable quantum photonics. Optics Letters, 2021, 46, 134.	3.3	10
26	Long Short-Term Memory Neural Network for Mitigating Transmission Impairments of 160 Gbit/s PAM4 Microring Modulation. , 2021, , .		9
27	Multi-functional photonic processors using coherent network of micro-ring resonators. APL Photonics, 2021, 6, .	5.7	12
28	Ultra-Compact Polarization Analyzer Based on Micro-Ring Resonators. IEEE Photonics Technology Letters, 2021, 33, 1371-1374.	2.5	2
29	Low-Threshold Continuous-Wave Anti-Stokes Raman Lasing in Silicon Racetrack Resonators. ACS Photonics, 2021, 8, 3462-3468.	6.6	1
30	Low crosstalk multi-mode crossing structure for multimode bound states in the continuum photonic circuits. , 2021, , .		0
31	Multimode Wavelength Division Demultiplexing Based on an Angled Multimode Interference Coupler. , 2021, , .		0
32	Multimode Waveguide Grating Couplers for Mode Division Multiplexing in Multi-mode fibers. , 2021, , .		0
33	Ultra-Broadband Hyperuniform Disordered Silicon Photonic Polarizers. IEEE Journal of Selected Topics in Quantum Electronics, 2020, 26, 1-9.	2.9	13
34	Efficient Mode Multiplexer for Few-Mode Fibers Using Integrated Silicon-on-Insulator Waveguide Grating Coupler. IEEE Journal of Quantum Electronics, 2020, 56, 1-7.	1.9	48
35	Enhanced four-wave mixing with MoS ₂ on a silicon waveguide. Journal of Optics (United) Tj ETQq1 1	0.784314 2.2	rgBT /Over
36	Ultracompact 40-Channel Arrayed Waveguide Grating on Silicon Nitride Platform at 860 nm. IEEE	1.9	16

Journal of Quantum Electronics, 2020, 56, 1-8.

#	Article	IF	CITATIONS
37	Pulse transit time based respiratory rate estimation with singular spectrum analysis. Medical and Biological Engineering and Computing, 2020, 58, 257-266.	2.8	7
38	Indium Phosphide Membrane Nanophotonic Integrated Circuits on Silicon. Physica Status Solidi (A) Applications and Materials Science, 2020, 217, 1900606.	1.8	33
39	An Experimental Demonstration of 160-Gbit/s PAM-4 Using a Silicon Micro-Ring Modulator. IEEE Photonics Technology Letters, 2020, 32, 125-128.	2.5	41
40	1.12-Tbit/s PAM-4 Enabled by a Silicon Photonic Transmitter Bridged With a 7-Channel MCF. IEEE Photonics Technology Letters, 2020, 32, 987-990.	2.5	8
41	Bound-States-in-Continuum Hybrid Integration of 2D Platinum Diselenide on Silicon Nitride for High-Speed Photodetectors. ACS Photonics, 2020, 7, 2643-2649.	6.6	32
42	Sub-milliwatt optical frequency combs in dual-pumped high-Q multimode silicon resonators. Applied Physics Letters, 2020, 117, .	3.3	9
43	High-speed infrared two-dimensional platinum diselenide photodetectors. Applied Physics Letters, 2020, 116, .	3.3	33
44	1.3ÂÂμm Quantum Dotâ€Distributed Feedback Lasers Directly Grown on (001) Si. Laser and Photonics Reviews, 2020, 14, 2000037.	8.7	40
45	Quantum Dot Lasers: Directly Modulated Singleâ€Mode Tunable Quantum Dot Lasers at 1.3µm (Laser) Tj ETQ	q1 <u>1</u> 0.78 8.7	4314 rgBT C
46	Radiation pressure and electrostriction induced enhancement for Kerr-like nonlinearities in a nanoscale silicon pedestal waveguide. Journal of Optics (United Kingdom), 2020, 22, 055502.	2.2	0
47	Quantum Dot Lasers: 1.3µm Quantum Dotâ€Distributed Feedback Lasers Directly Grown on (001) Si (Laser) T	j ETQq1 1 8.7	0.784314 rg
48	Directly Modulated Singleâ€Mode Tunable Quantum Dot Lasers at 1.3µm. Laser and Photonics Reviews, 2020, 14, 1900348.	8.7	24
49	Enhanced thermo-optic nonlinearities in a MoS ₂ -on-silicon microring resonator. Applied Physics Express, 2020, 13, 022004.	2.4	8
50	High-dimensional communication on etchless lithium niobate platform with photonic bound states in the continuum. Nature Communications, 2020, 11, 2602.	12.8	73
51	Quantum states of higher-order whispering gallery modes in a silicon micro-disk resonator. Journal of the Optical Society of America B: Optical Physics, 2020, 37, 2231.	2.1	6
52	High Efficiency, High Gain and High Saturation Output Power Quantum Dot SOAs Grown on Si and applications. , 2020, , .		9
53	Compact high-extinction tunable CROW filters for integrated quantum photonic circuits. Optics Letters, 2020, 45, 1289.	3.3	20
54	Bufferless III–V photodetectors directly grown on (001) silicon-on-insulators. Optics Letters, 2020, 45, 1754.	3.3	18

#	Article	IF	CITATIONS
55	Integrated Mikaelian Lens Implemented by Subwavelength Grating. , 2020, , .		Ο
56	High-dimensional communication on etchless lithium niobate platform with photonic bound states in the continuum. , 2020, , .		4
57	Hybrid two-dimensional-material photonics with bound states in the continuum. , 2020, , .		0
58	Graphene-silicon nitride photodetector with bound state in the continuum. , 2020, , .		0
59	1.3 qm tunable quantum dot lasers. , 2020, , .		1
60	Integrated Photon-Pair Generation and ~112 dB Pump Rejection Filters for Silicon Quantum Photonics. , 2020, , .		0
61	Silicon photonics for spatially multiplexed high capacity optical fiber communications. , 2020, , .		0
62	280 Gb/s Dual-Polarization Transmitter using Ge-on-Si EAMs for Short-Reach Interconnects. , 2020, , .		4
63	112 Gb/s 16-QAM OFDM for 80-km Data Center Interconnects Using Silicon Photonic Integrated Circuits and Kramers–Kronig Detection. Journal of Lightwave Technology, 2019, 37, 3532-3538.	4.6	10
64	InP membrane micro-ring resonator for generating heralded single photons. Journal of Optics (United) Tj ETQq0	0 0 rgBT / 2.2	Overlock 10 T
65	Hybrid 2Dâ€Material Photonics with Bound States in the Continuum. Advanced Optical Materials, 2019, 7, 1901306.	7.3	43
66	Ultra‧harp Multimode Waveguide Bends with Subwavelength Gratings. Laser and Photonics Reviews, 2019, 13, 1800119.	8.7	87
67	Mode-Division-Multiplexing (MDM) of 9.4-Tbit/s OFDM Signals on Silicon-on-Insulator (SOI) Platform. IEEE Access, 2019, 7, 129104-129111.	4.2	12
68	Integrated Plasmonic Infrared Photodetector Based on Colloidal HgTe Quantum Dots. Advanced Materials Technologies, 2019, 4, 1900354.	5.8	36
69	Entangled photon pair generation from an InP membrane micro-ring resonator. Applied Physics Letters, 2019, 114, .	3.3	28
70	A High Spur-Free Dynamic Range Silicon DC Kerr Ring Modulator for RF Applications. Journal of Lightwave Technology, 2019, 37, 3261-3272.	4.6	12
71	Subwavelength Engineering in Silicon Photonic Devices. IEEE Journal of Selected Topics in Quantum Electronics, 2019, 25, 1-13.	2.9	17
72	Integrated Silicon Photonics Remote Radio Frontend (RRF) for Single-Sideband (SSB) Millimeter-Wave Radio-Over-Fiber (ROF) Systems. IEEE Photonics Journal, 2019, 11, 1-8.	2.0	31

#	Article	IF	CITATIONS
73	High Resolution Silicon Nitride Spectrometer by Integrating Micro-Rings and Arrayed Waveguide Gratings in Tandem. , 2019, , .		2
74	Hyperuniform disordered photonic bandgap polarizers. Journal of Applied Physics, 2019, 126, .	2.5	12
75	General Scattering Matrix for Design of Linear Coherent Networks using Microring Resonators. , 2019, , .		Ο
76	High Resolution Silicon Nitride Spectrometer by Integrating Micro-Rings and Arrayed Waveguide Gratings in Tandem. , 2019, , .		0
77	Implementing Deep Neural Network for Signal Transmission Distortion Mitigation of PAM-4 Generated by Silicon Mach-Zehnder Modulator. , 2019, , .		1
78	Continuous-Wave Raman Lasing in Silicon Ring Resonator with Sub-Milliwatt Pump Threshold. , 2019, , .		1
79	Characteristics of 1.3μm Electrically Pumped InAs/AlGaInAs Quantum Dot Lasers on (001) Silicon. , 2019, ,		Ο
80	100 GHz colliding pulse mode locked quantum dot lasers directly grown on Si for WDM application. , 2019, , .		3
81	Dual-wavelength-band subwavelength grating coupler operating in the near infrared and extended shortwave infrared. Optics Letters, 2019, 44, 3621.	3.3	28
82	High-channel-count 20  GHz passively mode-locked quantum dot laser directly grown on Si with 41  Tbit/s transmission capacity. Optica, 2019, 6, 128.	9.3	129
83	High-speed van der Waals heterostructure tunneling photodiodes integrated on silicon nitride waveguides. Optica, 2019, 6, 514.	9.3	26
84	Photonic integrated circuits with bound states in the continuum. Optica, 2019, 6, 1342.	9.3	130
85	Two-dimensional van der Waals heterostructure tunneling photodiodes on silicon nitride waveguides. , 2019, , .		Ο
86	Hyperuniform Disordered Polarisers for the Mid-Infrared. , 2019, , .		0
87	80-km Transmission with Silicon Micro-Ring Modulators and Kramers-Kronig Direct Detection. , 2019, ,		2
88	Asymmetric graphene-on-silicon nitride waveguide photodetector towards fast speed and high responsivity. , 2019, , .		0
89	Terabit interconnects with a 20-GHz O-band passively mode locked quantum dot laser grown directly on silicon. , 2019, , .		Ο
90	Photon Pair Generation and Filtering Using Monolithically Integrated Silicon Micro-disk and Coupled Resonator Optical Waveguide. , 2019, , .		0

#	Article	IF	CITATIONS
91	Experimental demonstration of 1111-Gb/s net information rate using IM/DD probabilistically shaped orthogonal chirp-division multiplexing with a 10-GHz-class modulator. Optics Express, 2019, 27, 33789.	3.4	2
92	Compensation of Dispersion-Induced Power Fading in Analog Photonic Links by Gain-Transparent SBS. IEEE Photonics Technology Letters, 2018, 30, 688-691.	2.5	8
93	Fully suspended slot waveguide platform. Journal of Applied Physics, 2018, 123, .	2.5	33
94	2.6 Tbit/s On-Chip Optical Interconnect Supporting Mode-Division-Multiplexing and PAM-4 Signal. IEEE Photonics Technology Letters, 2018, 30, 1052-1055.	2.5	42
95	3 × 104 Gb/s Single-λ Interconnect of Mode-Division Multiplexed Network With a Multicore Fiber. Journal of Lightwave Technology, 2018, 36, 318-324.	4.6	24
96	10 hannel Mode (de)multiplexer with Dual Polarizations. Laser and Photonics Reviews, 2018, 12, 1700109.	8.7	210
97	A silicon nitride waveguide-integrated chemical vapor deposited graphene photodetector with 38 GHz bandwidth. Nanoscale, 2018, 10, 21851-21856.	5.6	20
98	Influence of Nonlinear Losses on Spontaneous Four Wave Mixing in InP Membrane Micro-ring Resonator. , 2018, , .		0
99	Compact and High-Speed Ge Franz-Keldysh I/Q Modulator Used with Kramers-Kronig Receiver. , 2018, , .		1
100	Electrically Tunable Terahertz Liquid Crystal Spatial Phase Shifter. , 2018, , .		0
101	Polarization Sensitive Plasmonic Photodetector Based on HgTe Quantum Dots. , 2018, , .		Ο
102	Hybrid Integration of Black Phosphorus-WSe <inf>2</inf> Heterojunction Photodetector on Silicon Waveguide. , 2018, , .		0
103	Low Crosstalk Bent Multimode Waveguide for On-chip Mode-Division Multiplexing Interconnects. , 2018, , .		11
104	High-Q germanium optical nanocavity. Photonics Research, 2018, 6, 925.	7.0	20
105	Integrated germanium-on-silicon Franz–Keldysh vector modulator used with a Kramers–Kronig receiver. Optics Letters, 2018, 43, 4333.	3.3	15
106	Graphene-on-silicon nitride waveguide photodetector with interdigital contacts. Applied Physics Letters, 2018, 112, 211107.	3.3	37
107	Machine Learning Adaptive Receiver for PAM-4 Modulated Optical Interconnection Based on Silicon Microring Modulator. Journal of Lightwave Technology, 2018, 36, 4106-4113.	4.6	24
108	Mid-infrared high-Q germanium microring resonator. Optics Letters, 2018, 43, 2885.	3.3	39

#	Article	IF	CITATIONS
109	Tailorable dual-wavelength-band coupling in a transverse-electric-mode focusing subwavelength grating coupler. Optics Letters, 2018, 43, 2985.	3.3	33
110	Negative Frequency-Chirped 112-Gb/s PAM-4 Using an Integrated Germanium Franz-Keldysh Modulator. IEEE Photonics Technology Letters, 2018, 30, 1443-1446.	2.5	7
111	High-performance chemical vapor deposited graphene-on-silicon nitride waveguide photodetectors. Optics Letters, 2018, 43, 1399.	3.3	33
112	Silicon-graphene photonic devices. Journal of Semiconductors, 2018, 39, 061009.	3.7	12
113	192-Gbit/s PAM-4 Optical Interconnect using Mode-Division Multiplexing. , 2018, , .		1
114	Efficient perfectly vertical grating coupler for multi-core fibers fabricated with 193  nm DUV lithography. Optics Letters, 2018, 43, 5709.	3.3	55
115	30-GHz graphene-on-silicon nitride waveguide photodetector. , 2018, , .		1
116	512-Gbit/s PAM-4 Signals Direct-Detection using Silicon Photonics Receiver with Volterra Equalization. , 2018, , .		2
117	Mid-infrared germanium photonic integrated circuits for on-chip biochemical sensing. , 2018, , .		0
118	Assessment of Integrated Ge Franz-Keldysh Modulator for Discrete Multi-Tone Modulation. , 2018, , .		1
119	Monolithic Dual-polarization Silicon Modulator for 180 Gb/s DMT Signal Transmission. , 2018, , .		0
120	112-Gb/s PAM-4 using Integrated Germanium on Silicon Franz Keldysh Modulator. , 2018, , .		2
121	Integrated Plasmonic Waveguide at the Mid-Infrared. , 2018, , .		1
122	Recent progress in nano-optomechanical devices at microwave frequencies. , 2018, , .		0
123	Mode-Division Multiplexing for Silicon Photonic Network-on-Chip. Journal of Lightwave Technology, 2017, 35, 3223-3228.	4.6	86
124	Synergistic Effects of Plasmonics and Electron Trapping in Graphene Short-Wave Infrared Photodetectors with Ultrahigh Responsivity. ACS Nano, 2017, 11, 430-437.	14.6	192
125	Pulse Transit Time Based Continuous Cuffless Blood Pressure Estimation: A New Extension and A Comprehensive Evaluation. Scientific Reports, 2017, 7, 11554.	3.3	149
126	Integrated near-infrared photodetector based on colloidal HgTe quantum dot loaded plasmonic waveguide. , 2017, , .		4

#	Article	IF	CITATIONS
127	High speed DPSK modulation up to 30 Gbps for short reach optical communications using a silicon microring modulator. , 2017, , .		1
128	Fully suspended mid-infrared racetrack resonator with subwavelength grating cladding. , 2017, , .		2
129	Scalable Ultra-Wideband Pulse Generation Based on Silicon Photonic Integrated Circuits. IEEE Photonics Technology Letters, 2017, 29, 1896-1899.	2.5	3
130	Mid-infrared germanium photonic crystal cavity. Optics Letters, 2017, 42, 2882.	3.3	27
131	Flat-top Frequency Comb Generation with Silicon Microring Modulator and Filter. , 2017, , .		8
132	Single-λ 312 Gb/s Discrete Multi-Tone Interconnect of Mode-Division Multiplexed Network with a Multicore Fiber. , 2017, , .		1
133	Fully suspended slot waveguides for high refractive index sensitivity. Optics Letters, 2017, 42, 1245.	3.3	42
134	Cavity-enhanced thermo-optic bistability and hysteresis in a graphene-on-Si_3N_4 ring resonator. Optics Letters, 2017, 42, 1950.	3.3	34
135	On-chip reconfigurable optical add-drop multiplexer for hybrid wavelength/mode-division-multiplexing systems. Optics Letters, 2017, 42, 2802.	3.3	66
136	Focusing subwavelength grating coupler for mid-infrared suspended membrane germanium waveguides. Optics Letters, 2017, 42, 2094.	3.3	76
137	Equalization of PAM-4 Signal Generated by Silicon Microring Modulator for 64-Gbit/s Transmission. Journal of Lightwave Technology, 2017, 35, 4943-4948.	4.6	14
138	Forward stimulated Brillouin scattering in silicon microring resonators. Applied Physics Letters, 2017, 111, .	3.3	9
139	Transmission Performance Improvement of PAM-4 Signal Direct-Detected by Ge-Si Photodiode using Volterra Equalization. , 2017, , .		1
140	Contribution of electrostriction and radiation pressure to Kerr-like nonlinearities in silicon pedestal waveguides. , 2017, , .		1
141	Fully suspended nanophotonic waveguide resonators with high quality factor and tailorable operational bandwidth. , 2017, , .		1
142	64-Gbit/s PAM-4 20-km Transmission Using Silicon Micro-ring Modulator for Optical Access Networks. , 2017, , .		9
143	Enhanced Thermo-Optic Bistability in Graphene-on-Silicon Nitride Ring Resonators. , 2017, , .		1
144	Monolithically integrated reconfigurable add-drop multiplexer for mode-division-multiplexing systems. Optics Letters, 2016, 41, 5298.	3.3	55

4

#	Article	IF	CITATIONS
145	128-Gb/s Line Rate OFDM Signal Modulation Using an Integrated Silicon Microring Modulator. IEEE Photonics Technology Letters, 2016, 28, 2058-2061.	2.5	23
146	Enhancement of self-phase modulation induced spectral broadening in silicon suspended membrane waveguides. Journal of Optics (United Kingdom), 2016, 18, 055503.	2.2	11
147	Design of Mid-infrared electro-optic modulators based on aluminum nitride waveguides. Journal of Lightwave Technology, 2016, , 1-1.	4.6	21
148	Nanophotonic structures for waveguide couplers and polarizers. , 2016, , .		0
149	A new modeling methodology for continuous cuffless blood pressure measurement. , 2016, , .		7
150	Multiplexing and switching for mode division multiplexed optical interconnects. , 2016, , .		0
151	A pulse transit time based fusion method for the noninvasive and continuous monitoring of respiratory rate. , 2016, 2016, 4240-4243.		4
152	Ultraviolet optomechanical crystal cavities with ultrasmall modal mass and high optomechanical coupling rate. Scientific Reports, 2016, 6, 37134.	3.3	5
153	A new design for coupling light between silicon strip waveguide and plasmonic slot waveguide. Proceedings of SPIE, 2016, , .	0.8	1
154	Narrow line-width single-longitudinal-mode fiber laser using silicon-on-insulator based micro-ring-resonator. Laser Physics Letters, 2016, 13, 025102.	1.4	6
155	High-responsivity graphene-on-silicon slot waveguide photodetectors. Nanoscale, 2016, 8, 13206-13211.	5.6	98
156	110 GHz hybrid mode-locked fiber laser with enhanced extinction ratio based on nonlinear silicon-on-insulator micro-ring-resonator (SOI MRR). Laser Physics Letters, 2016, 13, 035101.	1.4	11
157	Amplitude and Phase Modulation of UWB Monocycle Pulses on a Silicon Photonic Chip. IEEE Photonics Technology Letters, 2016, 28, 248-251.	2.5	10
158	Impact of heart disease and calibration interval on accuracy of pulse transit time–based blood pressure estimation. Physiological Measurement, 2016, 37, 227-237.	2.1	49
159	Hyperuniform Disordered Network Polarizers. IEEE Journal of Selected Topics in Quantum Electronics, 2016, 22, 288-294.	2.9	34
160	High Coupling Efficiency Silicon Waveguide to Metal–Insulator–Metal Waveguide Mode Converter. Journal of Lightwave Technology, 2016, 34, 2467-2472.	4.6	35
161	Continuous Cuffless Blood Pressure Estimation Using Pulse Transit Time and Photoplethysmogram Intensity Ratio. IEEE Transactions on Biomedical Engineering, 2016, 63, 964-972.	4.2	246

162 56 Gbit/s DMT Signal Generated by an Integrated Silicon Ring Modulator. , 2016, , .

#	Article	IF	CITATIONS
163	Mode Division Multiplexed 3 $ ilde{A}$ — 28 Gbit/s On-chip Photonic Interconnects. , 2016, , .		4
164	Photoresponse of Graphene-on-Silicon Nitride Microring Resonator. , 2016, , .		2
165	Photonic integration for Terabit scale single-wavelength on-chip Optical Interconnects. , 2016, , .		Ο
166	Enhanced optical Kerr nonlinearity of MoS_2 on silicon waveguides. Photonics Research, 2015, 3, 206.	7.0	58
167	High Responsivity, Broadband, and Fast Graphene/Silicon Photodetector in Photoconductor Mode. Advanced Optical Materials, 2015, 3, 1207-1214.	7.3	141
168	Graphene photodetector integrated on silicon nitride waveguide. Journal of Applied Physics, 2015, 117, .	2.5	46
169	Wavelength-tunable erbium-doped fiber laser using silicon-on-insulator (SOI) based micro-ring with narrow laser linewidth. , 2015, , .		Ο
170	Thermo-optic tunable silicon grating coupler. , 2015, , .		5
171	Graphene absorption enhancement using silicon slot waveguides. , 2015, , .		2
172	Graphene on Silicon-on-Sapphire Waveguide Photodetectors. , 2015, , .		2
173	Optical Absorption in Graphene-on-Silicon Nitride Microring Resonators. IEEE Photonics Technology Letters, 2015, 27, 1765-1767.	2.5	37
174	Optical Absorption and Thermal Nonlinearities in Graphene-on-Silicon Nitride Microring Resonators. , 2015, , .		4
175	Relaxation Dynamics of Optically Generated Carriers in Graphene-on-Silicon Nitride Waveguide Devices. , 2015, , .		2
176	Ultra-wideband monocycle pulses amplitude modulation based on integrated microring modulator. , 2015, , .		0
177	Enhanced self-phase modulation in silicon suspended membrane waveguides. , 2015, , .		Ο
178	Aluminum Nitride Electro-optic Modulator at Mid-IR Wavelengths. , 2015, , .		0
179	Silicon waveguide dispersion changes induced by graphene overlay. , 2014, , .		0
180	Scalable Optical Multicasting and Receiver for Networks- on-Chip. , 2014, , .		0

11

#	Article	IF	CITATIONS
181	Introduction for the Group-IV Photonics feature. Photonics Research, 2014, 2, GP1.	7.0	5
182	Experimental demonstration of polarization-insensitive air-cladding grating couplers for silicon-on-insulator waveguides. Optics Letters, 2014, 39, 2206.	3.3	73
183	A secure WDM ring access network employing silicon micro-ring based remote node. Optical Fiber Technology, 2014, 20, 336-340.	2.7	Ο
184	Optical Nyquist filters based on silicon coupled resonator optical waveguides. Optics Communications, 2014, 329, 23-27.	2.1	11
185	Stabilization of a multiwavelength erbium-doped fiber laser using a nonlinear silicon waveguide. Applied Physics B: Lasers and Optics, 2014, 114, 367-371.	2.2	12
186	Increase of the grating coupler bandwidth with a graphene overlay. Applied Physics Letters, 2014, 104, .	3.3	9
187	In-Plane Optical Absorption and Free Carrier Absorption in Graphene-on-Silicon Waveguides. IEEE Journal of Selected Topics in Quantum Electronics, 2014, 20, 43-48.	2.9	75
188	A 110 GHz passive mode-locked fiber laser based on a nonlinear silicon-micro-ring-resonator. Laser Physics Letters, 2014, 11, 065101.	1.4	17
189	Increasing the grating coupler bandwidth with a high numerical-aperture fiber. , 2014, , .		1
190	In-Plane Mid-Infrared Optical Absorption of Graphene on Silicon-on-Sapphire Waveguides. , 2014, , .		1
191	TWDM-PON With Signal Remodulation and Rayleigh Noise Circumvention for NG-PON2. IEEE Photonics Journal, 2013, 5, 7902306-7902306.	2.0	15
192	High-responsivity graphene/silicon-heterostructure waveguide photodetectors. Nature Photonics, 2013, 7, 888-891.	31.4	731
193	Mode-locked fiber laser using graphene on silicon waveguide. , 2013, , .		2
194	Polarization-Insensitive Phase-Preserving Regenerator Based on a Fiber Optical Parametric Amplifier With Dual Orthogonal Pumps. IEEE Photonics Technology Letters, 2013, 25, 362-364.	2.5	5
195	Apodized focusing subwavelength gratings for simultaneous coupling of TE and TM modes. , 2013, , .		0
196	100 GHz passive mode-locked laser based on nonlinear silicon microring resonator. , 2013, , .		1
197	250-GHz Passive Harmonic Mode-Locked Er-Doped Fiber Laser by Dissipative Four-Wave Mixing With Silicon-Based Micro-Ring. IEEE Photonics Journal, 2013, 5, 1502107-1502107.	2.0	26
198	Compatibility of Silicon Mach-Zehnder Modulators for Advanced Modulation Formats. Journal of Lightwave Technology, 2013, 31, 2550-2554.	4.6	46

#	Article	IF	CITATIONS
199	Stable and wavelength-tunable silicon-micro-ring-resonator based erbium-doped fiber laser. Optics Express, 2013, 21, 2869.	3.4	26
200	Multi-Bound Pulse State in a 250 GHz Mode-Locked Fiber Laser Based on a Silicon Micro-Ring Resonator. , 2013, , .		1
201	Spectral hole burning in silicon waveguides with a graphene layer on top. Optics Letters, 2013, 38, 1930.	3.3	9
202	UWB monocycle pulse generation based on colourless silicon photonic integrated circuit. Electronics Letters, 2013, 49, 1291-1293.	1.0	4
203	Polarization dependent loss of graphene-on-silicon waveguides. , 2013, , .		1
204	In-plane saturable absorption of graphene on silicon waveguides. , 2013, , .		2
205	Performance of silicon coupled resonator waveguides for integrated Nyquist filter. , 2013, , .		1
206	Focusing Subwavelength Grating Couplers. , 2013, , .		0
207	Amplitude Regeneration of 80-Gb/s Polarization-Multiplexed RZ-DPSK Signals in a Dual-Orthogonal-Pump Fiber Optical Parametric Amplifier. , 2013, , .		2
208	Demonstration of bi-directional LED visible light communication using TDD traffic with mitigation of reflection interference. Optics Express, 2012, 20, 23019.	3.4	65
209	Focusing subwavelength grating coupler for mid-infrared suspended membrane waveguide. Optics Letters, 2012, 37, 1217.	3.3	83
210	Demodulation of 20  Gbaud/s differential quadrature phase-shift keying signals using wavelength-tunable silicon microring resonators. Optics Letters, 2012, 37, 3462.	3.3	10
211	Investigation of 4-ASK modulation with digital filtering to increase 20 times of direct modulation speed of white-light LED visible light communication system. Optics Express, 2012, 20, 16218.	3.4	62
212	Tunable integrated variable bit-rate DPSK silicon receiver. Optics Letters, 2012, 37, 4738.	3.3	17
213	Wideband subwavelength gratings for coupling between silicon-on-insulator waveguides and optical fibers. Optics Letters, 2012, 37, 3483.	3.3	89
214	Broadband focusing grating couplers for suspended-membrane waveguides. Optics Letters, 2012, 37, 5181.	3.3	52
215	OSNR measurements using silicon grating coupler and integrated photodiode. , 2012, , .		1
216	Mid-infrared Suspended Membrane Waveguide and Ring Resonator on Silicon-on-Insulator. IEEE Photonics Journal, 2012, 4, 1510-1519.	2.0	151

#	Article	IF	CITATIONS
217	Apodized focusing subwavelength grating couplers for suspended membrane waveguides. Applied Physics Letters, 2012, 101, .	3.3	65
218	Mid-infrared suspended membrane waveguides on silicon-on-insulator. , 2012, , .		0
219	Characterization of Mid-Infrared Silicon-on-Sapphire Microring Resonators With Thermal Tuning. IEEE Photonics Journal, 2012, 4, 1095-1102.	2.0	26
220	Generation of Multichannel Delayed Pulses by Four-Wave-Mixing-Assisted Stimulated Brillouin Scattering Slow-Light System. IEEE Photonics Journal, 2012, 4, 1203-1211.	2.0	1
221	An Ultracompact OSNR Monitor Based on an Integrated Silicon Microdisk Resonator. IEEE Photonics Journal, 2012, 4, 1365-1371.	2.0	6
222	Design and applications of silicon waveguide grating couplers. Proceedings of SPIE, 2012, , .	0.8	7
223	Monolithic suspended membrane ring resonator for mid-infrared applications. , 2012, , .		0
224	Chromatic dispersion monitoring based on four wave mixing in silicon waveguide. , 2012, , .		0
225	Bit-Rate-Variable DPSK Demodulation Using Silicon Microring Resonators With Electro-Optic Wavelength Tuning. IEEE Photonics Technology Letters, 2012, 24, 1221-1223.	2.5	16
226	Dual-wavelength hybrid laser with micro-ring resonator and erbium-doped fiber amplifier. , 2012, , .		0
227	Four-wave mixing stabilized multiwavelength silicon/erbium-doped fiber hybrid ring laser. , 2012, , .		1
228	Comparison of extinction ratio enhancement of 10 and 40 Gb/s RZ-OOK signals using pump-modulated four-wave mixing in a silicon waveguide. , 2012, , .		0
229	Mid-Infrared Grating Couplers for Silicon-on-Sapphire Waveguides. IEEE Photonics Journal, 2012, 4, 104-113.	2.0	54
230	Demodulation of 40 Gb/s DPSK Signals Using a Silicon Microring Resonator with Electro-Optic Wavelength Tuning. , 2012, , .		0
231	Amplitude Noise Reduction, Pulse Format Conversion, and Wavelength Multicast of PSK Signal in a Fiber Optical Parametric Amplifier. , 2012, , .		0
232	Long-reach radio-over-fiber signal distribution using single-sideband signal generated by a silicon-modulator. Optics Express, 2011, 19, 11312.	3.4	31
233	Polarization-independent grating couplers for silicon-on-insulator nanophotonic waveguides. Optics Letters, 2011, 36, 796.	3.3	145
234	Device engineering for silicon photonics. NPG Asia Materials, 2011, 3, 34-40.	7.9	85

#	Article	IF	CITATIONS
235	Carrier Depletion Based Linear Silicon Modulator. , 2011, , .		3
236	OSNR Monitoring for NRZ-PSK Signals Using Silicon Waveguide Two-Photon Absorption. IEEE Photonics Journal, 2011, 3, 968-974.	2.0	10
237	Bi-wavelength two dimensional chirped grating couplers for low cost WDM PON transceivers. Optics Communications, 2011, 284, 2242-2244.	2.1	31
238	Bidirectional colorless wired and wireless WDM-PON with improved dispersion tolerance for radio over fiber. Optics Communications, 2011, 284, 3518-3521.	2.1	4
239	DQPSK demodulation using integrated silicon microring resonators. Optics Communications, 2011, 284, 172-175.	2.1	7
240	Mid-infrared micro-ring resonator on silicon-on-sapphire characterized by thermal tuning. , 2011, , .		1
241	Silicon waveguide side-cladding distributed Bragg reflector hybrid laser. , 2011, , .		1
242	Subwavelength Waveguide Grating Coupler for Fiber-to-Chip Coupling on SOI with 80nm 1dB-Bandwidth. , 2011, , .		5
243	Two dimensional silicon waveguide chirped grating couplers for vertical optical fibers. Optics Communications, 2010, 283, 2146-2149.	2.1	40
244	Long-Reach Multicast High Split-Ratio Wired and Wireless WDM-PON Using SOA for Remote Upconversion. IEEE Transactions on Microwave Theory and Techniques, 2010, 58, 3136-3143.	4.6	12
245	40-Gb/s Upstream Transmitters Using Directly Modulated 1.55-\$mu\$m VCSEL Array for High-Split-Ratio PONs. IEEE Photonics Technology Letters, 2010, 22, 347-349.	2.5	18
246	Apodized Waveguide Grating Couplers for Efficient Coupling to Optical Fibers. IEEE Photonics Technology Letters, 2010, 22, 1156-1158.	2.5	287
247	Rayleigh Backscattering Mitigation Using Wavelength Splitting for Heterogeneous Optical Wired and Wireless Access. IEEE Photonics Technology Letters, 2010, 22, 1294-1296.	2.5	24
248	Nonreciprocal Optical Modulation for Colorless Integrated Optical Transceivers in Passive Optical Networks. Journal of Optical Communications and Networking, 2010, 2, 131.	4.8	3
249	Characterization of Integrated Polarization-Diversity DPSK Demodulator with Two-Dimensional Chirped Grating Couplers and Ring Resonators. , 2010, , .		0
250	1.55-µm VCSEL transmission performance up to 20 Gb/s for access networks. , 2009, , .		4
251	Grating coupler for mid-infrared silicon-on-sapphire waveguide. , 2009, , .		3
252	Non-uniform focusing grating for coupling between silicon waveguide and vertical optical fiber. , 2009, , .		1

#	Article	IF	CITATIONS
253	Multi-channel mm-wave generation by frequency quadrupling using an optical modulator and a cascaded silicon microring filter. , 2009, , .		1
254	Characterization of deep etched holes arrays as grating couplers between optical fibers and nanophotonic waveguides. , 2009, , .		1
255	10-Gb/s colorless re-modulation of signal from 1550nm vertical cavity surface emitting laser array in WDM PON. , 2009, , .		1
256	Optical frequency doubling for multichannel radio-over-fibre system based on integrated phase modulator and silicon coupled microring notch filter. Electronics Letters, 2009, 45, 697.	1.0	8
257	Electroluminescence from metal–oxide–silicon tunneling diode with ion-beam-synthesized β-FeSi2 precipitates embedded in the active region. Nuclear Instruments & Methods in Physics Research B, 2009, 267, 1081-1084.	1.4	1
258	Mitigation of Signal Distortions Using Reference Signal Distribution With Colorless Remote Antenna Units for Radio-Over-Fiber Applications. Journal of Lightwave Technology, 2009, 27, 4773-4780.	4.6	19
259	Optical mm-Wave Signal Generation by Frequency Quadrupling Using an Optical Modulator and a Silicon Microresonator Filter. IEEE Photonics Technology Letters, 2009, 21, 209-211.	2.5	28
260	Etched Waveguide Grating Variable 1\$,imes,\$2 Splitter/Combiner and Waveguide Coupler. IEEE Photonics Technology Letters, 2009, 21, 268-270.	2.5	12
261	Optical Differential-Phase-Shift-Keying Demodulation Using a Silicon Microring Resonator. IEEE Photonics Technology Letters, 2009, 21, 295-297.	2.5	19
262	Nanoholes Grating Couplers for Coupling Between Silicon-on-Insulator Waveguides and Optical Fibers. IEEE Photonics Journal, 2009, 1, 184-190.	2.0	81
263	Chirped waveguide gratings for low-cost silicon photonic wire packaging and other applications. , 2009, , .		0
264	Correlation between impurities in Fe–Si amorphous layers synthesized by Fe implantation and photoluminescence property of β-FeSi2 precipitates in Si. Journal of Luminescence, 2008, 128, 1841-1845.	3.1	4
265	Nonlinear optical properties of silicon waveguides. Semiconductor Science and Technology, 2008, 23, 064007.	2.0	129
266	Fabrication-Tolerant Waveguide Chirped Grating Coupler for Coupling to a Perfectly Vertical Optical Fiber. IEEE Photonics Technology Letters, 2008, 20, 1914-1916.	2.5	122
267	WDM-PON Using Differential-Phase-Shift-Keying Remodulation of Dark Return-to-Zero Downstream Channel for Upstream. IEEE Photonics Technology Letters, 2008, 20, 833-835.	2.5	10
268	Colorless WDM-PON Optical Network Unit (ONU) Based on Integrated Nonreciprocal Optical Phase Modulator and Optical Loop Mirror. IEEE Photonics Technology Letters, 2008, 20, 863-865.	2.5	9
269	Characterization of silicon-on-insulator waveguide chirped grating for coupling to a vertical optical fiber. , 2008, , .		2
270	Chirped grating for efficient coupling from a silicon waveguide to a vertical optical fiber. , 2008, , .		2

#	Article	IF	CITATIONS
271	Surface morphology evolution of amorphous Fe–Si layers upon thermal annealing. Journal Physics D: Applied Physics, 2008, 41, 085418.	2.8	4
272	Differential Phase Shift Keying for Asynchronous Upstream Remodulation of Dark Return-to-Zero Downstream Channel. , 2008, , .		1
273	Rapid thermal annealing of ion beam synthesized β-FeSi2 nanoparticles in Si. Applied Physics Letters, 2008, 92, 211902.	3.3	12
274	Ion implantion in silicon waveguides for nonlinear effective length enhancement and power monitoring applications. , 2008, , .		0
275	DPSK Demodulation Using Mach-Zehnder Delay-Interferometer on Silicon-on-Insulator Integrated with Diffractive Grating Structure. , 2008, , .		2
276	Silicon Photonics Research in Hong Kong: Microresonator Devices and Optical Nonlinearities. IEICE Transactions on Electronics, 2008, E91-C, 156-166.	0.6	1
277	Non-reciprocal optical phase modulation for integrated NRZ/DPSK data re-modulation in optical access networks. , 2008, , .		Ο
278	Nonlinear response of silicon double-notch-shaped microdisk resonators with non-evanescent coupling. , 2008, , .		1
279	Photoresponse of \hat{l}^2 -FeSi<inf>2</inf> precipitates in a silicon waveguide. , 2007, , .		Ο
280	Non-evanescently pumped Raman silicon lasers using spiral-shaped microdisks. , 2007, , .		2
281	Time dependent density of free carriers generated by two photon absorption in silicon waveguides. Applied Physics Letters, 2007, 90, 211105.	3.3	49
282	Optical Burst and Transient Equalizer for 10Gb/s Amplified WDM-PON. , 2007, , .		2
283	Enhancement of Self Phase Modulation Induced Spectral Broadening in Silicon Waveguides by Ion Implantation. , 2007, , .		1
284	Non-evanescently pumped raman silicon lasers using spiral-shaped microdisks. , 2007, , .		0
285	Dynamic-channel-equalizer using in-line channel power monitor and electronic variable optical attenuator. Optics Communications, 2007, 272, 87-91.	2.1	5
286	3-bit/symbol optical modulation-demodulation simultaneously using DRZ, DPSK and PolSK. , 2006, , .		5
287	In-line channel power monitor based on helium ion implantation in silicon-on-insulator waveguides. IEEE Photonics Technology Letters, 2006, 18, 1882-1884.	2.5	55
288	Nonlinear absorption and Raman gain in helium-ion-implanted silicon waveguides. Optics Letters, 2006, 31, 1714.	3.3	71

#	Article	IF	CITATIONS
289	Nonlinear polarization rotation in a dispersion-flattened photonic-crystal fiber for ultrawideband (>100 nm) all-optical wavelength conversion of 10 Gbit/s nonreturn-to-zero signals. Optics Letters, 2006, 31, 1782.	3.3	12
290	Optical label switching of DRZ/DPSK orthogonal signal generated by photonic-crystal fiber. Optics Letters, 2006, 31, 2535.	3.3	4
291	3-bit/symbol optical data format based on simultaneous DRZ, DPSK and PolSK orthogonal modulations. Optics Express, 2006, 14, 1720.	3.4	2
292	Dynamic gain-tilt compensation using electronic variable optical attenuators and a thin film filter spectral tilt monitor. Optics Express, 2006, 14, 9022.	3.4	0
293	Bilevel mode converter between a silicon nanowire waveguide and a larger waveguide. Journal of Lightwave Technology, 2006, 24, 2428-2433.	4.6	39
294	Essential function of Smad3, but not Smad2, in TGF-beta-induced transcription of cell differentiation protein Id1. Journal of Surgical Research, 2006, 130, 171-172.	1.6	0
295	High speed logic gate using two-photon absorption in silicon waveguides. Optics Communications, 2006, 265, 171-174.	2.1	96
296	Simultaneous Four Channels Modulation Format Conversion in a Nonlinear Optical Loop Mirror with Suppressed Four-Wave-Mixing Crosstalk. , 2006, , .		0
297	Silicon Waveguides Based Ultra-wide-band Filter for Raman Amplification. , 2006, , .		0
298	Nonlinear self-distortion of picosecond optical pulses in silicon wire waveguides. , 2006, , .		1
299	Raman gain in helium ion implanted silicon waveguides. , 2006, , .		4
300	Helium Implantation into Silicon: Nonlinear and Linear Optoelectronic Applications. , 2006, , .		0
301	Multiple-wavelength Dynamic Gain Transient Compensation Based on Silicon Platform. , 2006, , .		0
302	High extinction-ratio orthogonal label switching of DRZ/DPSK generated by photonic crystal fiber. , 2006, , .		0
303	Wavelength Combiner based on Silicon Platform. , 2006, , .		0
304	Cross Gain Modulation in Asymmetrical Multi-Quantum Well Semiconductor Optical Amplifier. , 2006, , .		0
305	EDFA Per-Band Gain-Tilt Compensation. , 2006, , .		1
306	Theoretical analysis of continuous-wave Raman gain/lasing in silicon wire waveguides without carrier extraction scheme. IEICE Electronics Express, 2005, 2, 440-445.	0.8	8

#	Article	IF	CITATIONS
307	Enhanced infrared responsivity of helium implanted SOI waveguides. , 2005, , .		Ο
308	Transient gain dynamics in gain-clamped EDFA with different erbium dopant levels. , 2005, , .		1
309	Two-node demonstration of optical labeling using half-bit delayed dark RZ payload and DPSK label. , 2005, , .		1
310	Silicon-on-insulator optical waveguides: nonlinear properties and functional elements. , 2005, , .		0
311	Optical label encoding and swapping using half-bit delayed dark RZ payload and DPSK label. Optics Express, 2005, 13, 5325.	3.4	14
312	Ultrafast all-optical switching by cross-absorption modulation in silicon wire waveguides. Optics Express, 2005, 13, 7298.	3.4	120
313	Minimizing gain transient dynamics by optimizing the erbium concentration and cavity length of a gain clamped EDFA. Optics Express, 2005, 13, 7520.	3.4	1
314	Integrated polarization beam splitter in high index contrast silicon-on-insulator waveguides. IEEE Photonics Technology Letters, 2005, 17, 393-395.	2.5	132
315	Reduction of amplitude transients and BER of direct Modulation laser using birefringent fiber loop. IEEE Photonics Technology Letters, 2005, 17, 693-695.	2.5	13
316	Polarization-independent DPSK demodulation using a birefringent fiber loop. IEEE Photonics Technology Letters, 2005, 17, 1313-1315.	2.5	48
317	Orthogonal label switching using polarization-shift-keying payload and amplitude-shift-keying label. IEEE Photonics Technology Letters, 2005, 17, 2475-2477.	2.5	12
318	Gain Tilt Monitoring of EDFA by Optical Filtering Techniques. , 2005, , .		0
319	Nonlinearities in silicon-on-insulator optical waveguides. , 2005, , .		Ο
320	Nonlinear Absorption and Raman Scattering in Silicon-on-Insulator Optical Waveguides. IEEE Journal of Selected Topics in Quantum Electronics, 2004, 10, 1149-1153.	2.9	78
321	Filtering directly modulated laser diode pulses with a Mach-Zehnder optical delay interferometer. Electronics Letters, 2004, 40, 938.	1.0	6
322	All-Optical ASK/DPSK Label-Swapping and Buffering Using Fabry–Perot Laser Diodes. IEEE Journal of Selected Topics in Quantum Electronics, 2004, 10, 363-370.	2.9	27
323	Reduction of bit-pattern dependent errors from a semiconductor optical amplifier using an optical delay interferometer. Optics Communications, 2004, 232, 245-249.	2.1	11
324	High repetition rate pulses generated by differential phase assisted injection-locking of Fabry–Perot laser diode. Optics Communications, 2004, 241, 437-442.	2.1	0

#	Article	IF	CITATIONS
325	Efficient Raman amplification in silicon-on-insulator waveguides. Applied Physics Letters, 2004, 85, 3343-3345.	3.3	124
326	Improvement of Directly Modulated Diode-Laser Pulses Using an Optical Delay Interferometer. IEEE Photonics Technology Letters, 2004, 16, 632-634.	2.5	6
327	Role of free carriers from two-photon absorption in Raman amplification in silicon-on-insulator waveguides. Applied Physics Letters, 2004, 84, 2745-2747.	3.3	228
328	Manipulation of polarization-dependent effects by magnetostrictive stress on silicon-on-insulator rib waveguides. Applied Optics, 2004, 43, 6323.	2.1	2
329	All-Optical Modulation Format Conversion and Multicasting Using Injection-Locked Laser Diodes. Journal of Lightwave Technology, 2004, 22, 2386-2392.	4.6	30
330	Optical packet labeling based on simultaneous polarization shift keying and amplitude shift keying. Optics Letters, 2004, 29, 1861.	3.3	23
331	External-pump-free polarization-insensitive wavelength converter with fast wavelength switching using orthogonal pumps four-wave mixing in a semiconductor optical amplifier. IEEE Journal of Selected Topics in Quantum Electronics, 2004, 10, 1197-1202.	2.9	2
332	All-optical time-division demultiplexing with simultaneous regeneration in gain-switched distributed feedback lasers. Optics Communications, 2003, 226, 227-231.	2.1	1
333	All-optical RZ to NRZ data format and wavelength conversion using an injection locked laser. Optics Communications, 2003, 223, 309-313.	2.1	11
334	Polarization-independent time-division demultiplexing using orthogonal-pumps four-wave mixing. IEEE Photonics Technology Letters, 2003, 15, 129-131.	2.5	11
335	Polarization-independent wavelength conversion at 10 Gb/s using birefringence switching in a semiconductor optical amplifier. IEEE Photonics Technology Letters, 2003, 15, 87-89.	2.5	9
336	Mode conversion and birefringence adjustment by focused-ion-beam etching for slanted rib waveguide walls. Optics Letters, 2003, 28, 2109.	3.3	8
337	All-optical time-division demultiplexing with polarization-diversity nonlinear loop interferometer. Optics Express, 2003, 11, 2047.	3.4	5
338	Photovoltage detection of x-ray absorption and magnetic circular dichroism spectra of magnetic films grown on semiconductors. Journal of Applied Physics, 2003, 93, 2028-2033.	2.5	3
339	All-optical data-format and wavelength-conversion in two-wavelength injection-locked slave Fabry-Perot laser diodes. Electronics Letters, 2003, 39, 997.	1.0	10
340	Polarisation-insensitive widely tunable wavelength converter using polarisation-diversified SOA fibre-ring laser. Electronics Letters, 2003, 39, 96.	1.0	3
341	Widely tunable wavelength converter using a double-ring fiber laser with a semiconductor optical amplifier. IEEE Photonics Technology Letters, 2002, 14, 1445-1447.	2.5	35
342	Silicon waveguide two-photon absorption detector at 1.5 μm wavelength for autocorrelation measurements. Applied Physics Letters, 2002, 81, 1323-1325.	3.3	141

#	Article	IF	CITATIONS
343	Widely tunable all-optical wavelength converter using a fiber ring cavity incorporating a semiconductor optical amplifier. Optics Communications, 2002, 203, 101-106.	2.1	10
344	All-optical NRZ to RZ format and wavelength converter by dual-wavelength injection locking. Optics Communications, 2002, 209, 329-334.	2.1	49
345	Optical dispersion, two-photon absorption and self-phase modulation in silicon waveguides at 1.5â€,μm wavelength. Applied Physics Letters, 2002, 80, 416-418.	3.3	353
346	High extinction ratio wavelength conversion at 10â€Cbitâ^•s using birefringence switching in semiconductor optical amplifier. Electronics Letters, 2002, 38, 897.	1.0	5
347	<title>All-optical wavelength conversion using active semiconductor devices</title> ., 2001, , .		5
348	Polarisation-insensitive widely tunable wavelength converter using a single semiconductor optical amplifier. Electronics Letters, 2000, 36, 152.	1.0	22
349	Widely tunable polarization-independent all-optical wavelength converter using a semiconductor optical amplifier. IEEE Photonics Technology Letters, 2000, 12, 525-527.	2.5	27
350	Wavelength-tunable 40 GHz pulse-train generation using 10 GHz gain-switched Fabry-Perot laser and semiconductor optical amplifier. Electronics Letters, 2000, 36, 1580.	1.0	15
351	Photoconductive detection of millimeter waves using proton implanted GaAs. Applied Physics Letters, 1999, 75, 745-747.	3.3	2
352	Chirp reduction for arbitrary pulses by amplified chirped-pulse self-phase modulation in dispersion-shifted fiber. Optics Communications, 1999, 160, 109-113.	2.1	0
353	Etched cavity InGaAsP-InP waveguide Fabry-Perot filter tunable by current injection. Journal of Lightwave Technology, 1999, 17, 1890-1895.	4.6	16
354	Experimental characterization of dual-wavelength injection-locking of a Fabry–Perot laser diode. Optics Communications, 1998, 156, 321-326.	2.1	20
355	Fibre dispersion or pulse spectrum measurement using a sampling oscilloscope. Electronics Letters, 1997, 33, 983.	1.0	129
356	Laplacian pulse width, rms chirp, and their applications. Journal of the Optical Society of America B: Optical Physics, 1996, 13, 2464.	2.1	5
357	Two new transform-limited criteria and their applications in ultrafast optics and soliton systems. IEEE Journal of Quantum Electronics, 1996, 32, 2064-2070.	1.9	4
358	High sensitivity autocorrelation using two-photon absorption in InGaAsP waveguides. Electronics Letters, 1995, 31, 1773-1775.	1.0	29
359	Transverse offset loss between two identical noncircular single-mode waveguides. Applied Optics, 1995, 34, 5343.	2.1	2
360	First demonstration of two photon absorption in a semiconductor waveguide pumped by a diode laser. Electronics Letters, 1993, 29, 1660.	1.0	6

#	Article	IF	CITATIONS
361	Allâ€optical modulation with ultrafast recovery at low pump energies in passive InGaAs/InGaAsP multiquantum well waveguides. Applied Physics Letters, 1993, 62, 1451-1453.	3.3	23
362	Repression and speed improvement of photogenerated carrier induced refractive nonlinearity in InGaAs/InGaAsP quantum well waveguide. Electronics Letters, 1991, 27, 1447.	1.0	8
363	GaAs/GaAlAs multiquantum well waveguides for all-optical switching at 1.55 μm. Electronics Letters, 1991, 27, 1993.	1.0	12
364	Twoâ€photon absorption and selfâ€phase modulation in InGaAsP/InP multiâ€quantumâ€well waveguides. Journal of Applied Physics, 1991, 70, 3992-3994.	2.5	43
365	Polarization and field dependent twoâ€photon absorption in GaAs/AlGaAs multiquantum well waveguides in the halfâ€band gap spectral region. Applied Physics Letters, 1991, 59, 3440-3442.	3.3	14
366	High performance QCSE phase modulator for the 1.5–1.55 μm fibre band. Electronics Letters, 1990, 26, 1421.	1.0	8
367	Polarisation dependent optical modulation using the plasma effect in a GaAs-GaAlAs quantum well waveguide. Optics Communications, 1990, 74, 365-369.	2.1	5
368	Efficient InGaAsP/InP multiple quantum well waveguide optical phase modulator. Applied Physics Letters, 1990, 57, 2285-2287.	3.3	20
369	Broadband Wavelength Conversion in Semiconductor Optical Amplifier with Non-identical Multiple Quantum Wells. , 0, , .		1
370	TE/TM mode conversion in silicon waveguides using selective stress applying oxide patches and etched oxide windows. , 0, , .		1
371	Silicon-on-Insulator Waveguide Mach-Zehnder Wavelength Combiner. , 0, , .		0
372	Birefringent Fiber Loop to Improve Directly Modulated Laser Diode Pulses. , 0, , .		0
373	Ultrafast non-inverting wavelength conversion by cross-absorption modulation in silicon wire waveguides. , 0, , .		3